

Subcortical neuromorphometry in schizophrenia spectrum and bipolar disorders



Daniel Mamah^{a,*}, Kathryn I. Alpert^d, Deanna M. Barch^{a,b,c}, John G. Csernansky^d, Lei Wang^d

^aDepartment of Psychiatry, Washington University Medical School, St. Louis, United States

^bDepartment of Psychology, Washington University Medical School, St. Louis, United States

^cDepartment of Radiology, Washington University Medical School, St. Louis, United States

^dDepartment of Psychiatry and Behavioral Sciences, Northwestern University Feinberg School of Medicine, Chicago, United States

ARTICLE INFO

Article history:

Received 27 January 2016

Received in revised form 17 February 2016

Accepted 19 February 2016

Available online 23 February 2016

Keywords:

Schizophrenia

Bipolar

Schizoid personality

Shape

Hippocampus

Amygdala

Basal ganglia

Thalamus

ABSTRACT

Background: Disorders within the schizophrenia spectrum genetically overlap with bipolar disorder, yet questions remain about shared biological phenotypes. Investigation of brain structure in disease has been enhanced by developments in shape analysis methods that can identify subtle regional surface deformations. Our study aimed to identify brain structure surface deformations that were common across related psychiatric disorders, and characterize differences.

Methods: Using the automated FreeSurfer-initiated Large Deformation Diffeomorphic Metric Mapping, we examined volumes and shapes of seven brain structures: hippocampus, amygdala, caudate, nucleus accumbens, putamen, globus pallidus and thalamus. We compared findings in controls (CON; $n = 40$), and those with schizophrenia (SCZ; $n = 52$), schizotypal personality disorder (STP; $n = 12$), psychotic bipolar disorder (P-BP; $n = 49$) and nonpsychotic bipolar disorder (N-BP; $n = 24$), aged 15–35. Relationships between morphometric measures and positive, disorganized and negative symptoms were also investigated.

Results: Inward deformation was present in the posterior thalamus in SCZ, P-BP and N-BP; and in the subiculum of the hippocampus in SCZ and STP. Most brain structures however showed unique shape deformations across groups. Correcting for intracranial size resulted in volumetric group differences for caudate ($p < 0.001$), putamen ($p < 0.01$) and globus pallidus ($p < 0.001$). Shape analysis showed dispersed patterns of expansion on the basal ganglia in SCZ. Significant clinical relationships with hippocampal, amygdalar and thalamic volumes were observed.

Conclusions: Few similarities in surface deformation patterns were seen across groups, which may reflect differing neuropathologies. Posterior thalamic contraction in SCZ and BP suggest common genetic or environmental antecedents. Surface deformities in SCZ basal ganglia may have been due to antipsychotic drug effects.

© 2016 The Authors. Published by Elsevier Inc. This is an open access article under the CC BY-NC-ND license (<http://creativecommons.org/licenses/by-nc-nd/4.0/>).

1. Introduction

The term *schizophrenia spectrum disorder* has been used to describe a range of psychiatric conditions, including schizophrenia (SCZ), that share some genetic risk variants and clinical manifestations (Mamah and Barch, 2011). Among these, schizotypal personality disorder (STP) is the most commonly included in studies of the spectrum. This condition is typically not associated with florid psychotic symptoms of schizophrenia (such as hallucinations and bizarre delusions), but rather cognitive or perceptual distortions and eccentricities in everyday behavior. Bipolar disorder (BP) is not traditionally included among the schizophrenia spectrum disorders, despite the fact that genetic and

familial overlap is present with SCZ (Cardno and Owen, 2014). Psychotic bipolar disorder (P-BP) has clinical similarities with SCZ and also has been reported to more closely overlap genetically with SCZ compared to nonpsychotic bipolar disorder (N-BP). Notwithstanding the relationship across these disorders, few studies have compared their brain structure (Mamah et al., 2009). Such studies would provide information on the extent of similarities between disorders, and help clarify the phenotypic manifestations of specific genetic profiles.

Volumetric analyses of structural brain imaging data have been a mainstay of brain structure investigations in psychiatry. In recent years, developments in shape analysis methodology have led to structural measures that can supplement data derived from volumetric analysis. In studies of disease, investigation of the three-dimensional surfaces of brain subcortical structures have been shown to identify group abnormalities where the volumetric analysis did not, indicating that subtle surface abnormalities are more sensitive to shape than size

* Corresponding author at: Department of Psychiatry, Washington University Medical School, 660 S. Euclid, Saint Louis, MO 63110, United States.

E-mail address: mamahd@psychiatry.wustl.edu (D. Mamah).

(Mamah et al., 2009). Since shape analysis enables the uncovering of localized deformations on the surface of a brain structure, it may more precisely identify impaired pathways within the brain. This is particularly important in the study of brain structures with explicit regional differentiation in function, such as the thalamus (Sherman and Guillery, 2013) or striatum (Verstynen et al., 2012; Draganski et al., 2008; Lehericy et al., 2004). Previous shape analyses have been conducted in psychiatric patients, including those with SCZ (Mamah et al., 2009; Csernansky et al., 2004; Smith et al., 2011; Danivas et al., 2013; Kang et al., 2008; Csernansky et al., 2002; Mamah et al., 2012; Johnson et al., 2013; Qiu et al., 2010; Zierhut et al., 2013; Styner et al., 2004; Shenton et al., 2002; Mamah et al., 2008; Mamah et al., 2007; Ballmaier et al., 2008) BP (Qiu et al., 2013; Hwang et al., 2006; Womer et al., 2014; Ong et al., 2012; Liberg et al., 2014; Liberg et al., 2015) or STP (Levitt et al., 2009; Levitt et al., 2004) often with varying results. However, studies are often conducted using differing recruitment criteria, scanners, imaging protocols and analyses methodology, which can significantly influence results. Thus, investigating various diagnostic patient groups in a single study, with identical protocol, is therefore necessary to obtain valid comparisons. Our shape analysis represents the most extensive investigation of its kind to our knowledge, comparing multiple subcortical brain structures across several diagnostic groups. We used an automated shape analysis methodology involving Large Deformation Diffeomorphic Metric Mapping (LDDMM) that has been validated and previous applied in the evaluation of disease (Khan et al., 2008; Ceyhan et al., 2011; Qiu et al., 2009).

In the current study, we investigated the volumes and shapes of seven subcortical structures simultaneously (i.e. the hippocampus, amygdala, caudate, putamen, globus pallidus, nucleus accumbens, and thalamus). We compared findings in healthy controls to those of individuals with SCZ, psychotic (P-BP) and nonpsychotic (N-BP) bipolar disorder, and STP, obtained using the same MRI scanner, imaging protocol and analysis methodology. We hypothesize that overlapping structural abnormalities will exist across these groups, with SCZ most affected. Abnormalities are expected to be largely trend toward shrinkage, and be best captured by shape analysis. Due to a probable past history of typical antipsychotic drug use, we hypothesize that the basal ganglia in SCZ will be enlarged.

2. Materials and methods

2.1. Participants

The study was approved by the Institutional Review Board of Washington University. Participant groups included: 1) healthy controls (CON; $n = 40$); 2) bipolar disorder (BP; $n = 73$); 3) schizophrenia (SCZ; $n = 52$); and 4) schizotypal personality disorder (STP; $n = 12$). Participants' ages ranged between 15 and 35 yrs. Participants were recruited through targeted advertisements in local psychiatric clinics, hospitals, and newspapers and through the Washington University volunteers for health recruitment system. All participants gave written informed consent for participation. SCZ and BP participants were all outpatients, and clinically stable for at least two weeks. They were diagnosed on the basis of a consensus between a research psychiatrist and a trained research assistant who used the Structured Clinical Interview for DSM-IV Axis I Disorders (SCID-I). The Structured Clinical Interview for DSM-IV Axis II Disorders (SCID-II) was used to ascertain group diagnosis in STP participants. CON subjects were required to have no lifetime history of Axis I psychotic or mood disorders. Participants were excluded if they: (a) met DSM-IV criteria for substance dependence or severe/moderate abuse during the prior 6 months; (b) had a clinically unstable or severe general medical disorder; or (c) had a history of head injury with documented neurological sequelae or loss of consciousness. BP participants were subdivided into psychotic bipolar disorder (P-BP; $N = 49$) and nonpsychotic bipolar disorder (N-BP; $N = 24$) based on the presence or absence of a lifetime history of hallucinations and/or

non-grandiose delusions using the SCID-I. Demographic data are shown in Table 1.

2.2. Clinical assessment

Psychopathology was assessed by trained Masters level research assistants using the Scale for the Assessment of Negative Symptoms (SANS) and the Scale for the Assessment of Positive Symptoms (SAPS) (Andreasen et al., 1995). Specific subscale scores were summed to derive measures of positive symptoms (i.e. hallucination and delusion subscales), disorganization (i.e. formal thought disorder, bizarre behavior and attention subscales), and negative symptoms (i.e. flat affect, avolition, anhedonia and amotivation subscales).

2.3. Image acquisition and surface mapping

Magnetic Resonance (MR) scans were obtained using a Siemens (Erlangen, Germany) 3T Tim TRIO Scanner at Washington University Medical School. T1-weighted images were acquired using a sagittal MPRAGE 3D sequence (TR = 2400 ms, TE = 3.16 ms, flip = 8°; voxel size = $1 \times 1 \times 1$ mm).

Surfaces of the hippocampus, amygdala, basal ganglia (i.e. caudate, nucleus accumbens, putamen and globus pallidus), and thalamus were automatically generated using FS + LDDMM, as previously described (Khan et al., 2008). In brief, this method combines a probabilistic voxel-based classification method of FreeSurfer (Desikan et al., 2006) and a deformable template-based method of large deformation diffeomorphic metric mapping (LDDMM) (Beg et al., 2005). The initial subcortical segmentations for the hippocampus, amygdala, basal ganglia and thalamus were obtained from FreeSurfer version 5.3.0, followed by image registration with LDDMM that produced smooth transformations for each region of interest (ROI). A previously-published template based on a healthy volunteer was used (Wang et al., 2008) to derive the segmentations and surfaces. Subcortical segmentations for the hippocampus and thalamus also included boundaries demarcating constituent subfields. Each ROI volume was calculated as the enclosed volume of the mapped surface. Intracranial volume, total gray matter volume and cortical white matter volume were obtained directly from the FreeSurfer pipeline output.

2.4. Statistical analyses

Statistical analyses (excluding shape) were done using SAS 9.4 (SAS Institute Inc., Cary, NC). Repeated measures ANCOVA (covaried for age and sex) were used to investigate volumetric group differences in subcortical brain regions, using hemisphere as the repeated measure. To

Table 1
Demographics table.

Characteristics	Control ($n = 40$)	SCZ ($n = 52$)	Schizotypal ($n = 12$)	PBP ($n = 49$)	NPBP ($n = 24$)
Age – Mean (SD)	24.9 (5.0)	26.1 (4.1)	22.4 (3.5)	25.2 (3.6)	26.2 (3.7)
Sex – N (%)					
Female	20 (50.0)	14 (26.9)	5 (45.5)	29 (59.2)	16 (66.7)
Male	20 (50.0)	38 (73.1)	6 (54.5)	20 (40.8)	8 (33.3)
Race (%)					
Asian	2 (5.0)	0	0	1 (2.0)	2 (8.3)
Black	21 (52.5)	27 (51.9)	3 (27.3)	13 (26.5)	2 (8.3)
Hispanic	0	0	0	3 (6.1)	0
White	17 (42.5)	25 (48.1)	8 (72.7)	30 (61.2)	18 (75.0)
Mixed/other	0	0	0	2 (4.1)	2 (8.3)
Handedness					
Right	36 (90.0)	50 (96.2)	9 (81.8)	45 (91.8)	21 (87.5)
Left	4 (10.0)	2 (3.8)	2 (18.2)	4 (8.2)	3 (12.5)

investigate volumetric effects relative to brain size, intracranial volume was also included as a covariate in specific analyses. Relationships with volumes were explored using Pearson correlations, partialling out diagnosis, age and sex.

To compare structural shape across groups, surface displacement maps were first generated by computing the surface-normal component of the displacement of each surface vertex relative to the overall average for every participant. Then, pairwise group differences were examined using SurfStat, (Chung et al., 2010; Worsley et al., 2009) comparing each clinical group with CON. For each group pair, a linear mixed-effects model was performed at each vertex, modeling the displacement and using group, age and sex as the independent predictors. This produced a coefficient estimate and pooled standard error for group, from which a t-statistic was calculated. Significance was corrected for multiple comparisons by applying random field theory (RFT), (Adler, 1981; Adler and Hasofer, 1976) and visualized as a color map on the overall average surface. RFT on surfaces was an extension of the body of work by Worsley and colleagues on detecting functional MRI activation in 3-dimensional volumetric data (Worsley et al., 1999; Taylor and Worsley, 2007). Multiple comparison correction methods such as Bonferroni or false discovery rate (FDR) (Genovese et al., 2002) are not appropriate because certain properties of the neuroimaging data are not considered by these methods (Perneger, 1998). Namely, signals on adjacent vertices are correlated; signals may be spatially continuous (i.e., forming clusters) therefore the spatial extent of the signals must be considered in addition to peaks. RFT considers both peaks and spatial extent of the signal by modeling the noise as Gaussian random fields (Worsley, 2005; Chumbley and Friston, 2009). The topology is described by the expected Euler characteristic, which at high thresholds of the unadjusted p-value, becomes the expected number of clusters and approximates the family-wide error rate (FWER). On the surface, the expected Euler characteristic is calculated in terms of a search area, a roughness matrix and a given unadjusted p-value. The first two terms can be expressed together as counts of *resel* (resolution element), where *resel* is defined by the FWHM filter used to smooth the surface data. Then for a given unadjusted highly significant p-value at the vertex level, the Euler characteristic is the number of clusters, and the expected Euler characteristic approximates the adjusted p-value at the cluster level.

3. Results

3.1. Intracranial, gray matter and white matter volumes

Intracranial volumes showed a significant group effect ($F = 3.6$; $p = 0.008$). Least squared (controlling for age and sex) means of intracranial volumes were (in mm^3): 1,518,123 for CON; 1,486,408 for SCZ; 1,525,578 for STP; 1,598,787 for P-BP; and 1,556,028 for N-BP. Post hoc analyses showed significant differences between SCZ and P-BP ($p = 0.0004$).

Total gray matter volumes showed a significant group effect ($F = 3.9$; $p = 0.005$). Least squared means of total gray matter volumes were (in mm^3): 653,545 for CON; 622,722 for SCZ; 649,297 for STP; 667,948 for P-BP; and 660,335 for N-BP. Post hoc analyses showed significant differences between CON and SCZ ($p = 0.01$); SCZ and P-BP ($p = 0.0002$); and SCZ and N-BP ($p = 0.01$).

Total white matter volumes did not show a significant group effect ($F = 1.8$; $p = 0.14$).

3.2. Hippocampus volume and shape

Hippocampal and other subcortical volumes are shown in Table 2. After controlling for age and sex, there were no significant group effects. Including total intracranial volume as a covariate did not change non-significant group effects.

Hemispheric effects were significant ($p < 0.0001$), but there was no group by hemisphere effect. Left hippocampi were smaller than right hippocampi. Shape analysis of the hippocampus resulted in significant group differences, as shown in Fig. 1A. Notable surface deformations in the hippocampus and other subcortical structures, across groups, are also displayed in Table 3.

3.3. Amygdala volume and shape

There were no significant group differences in amygdala volumes. No significant group differences were present, with or without including total intracranial volume as a covariate. There were also no

Table 2
Subcortical volumes.

Region	Control (n = 40)	SCZ (n = 52)	Schizotypal (n = 12)	PBP (n = 49)	NPBP (n = 24)	F	p
Hippocampus							
Left							
Absolute	2418	2330	2417	2512	2443	2.2	0.07
Relative	2441	2396	2431	2431	2421	0.1	0.98
Right							
Absolute	2799	2742	2794	2903	2869		
Relative	2827	2820	2811	2807	2843		
Amygdala							
Left							
Absolute	1350	1315	1326	1386	1340	1.7	0.16
Relative	1364	1354	1334	1338	1327	0.4	0.81
Right							
Absolute	1392	1352	1376	1439	1391		
Relative	1405	1390	1385	1392	1377		
Caudate							
Left							
Absolute	3549	3581	3399	3595	3432	1.0	0.43
Relative	3588	3690	3422	3460	3396	4.6	0.001*
Right							
Absolute	3516	3555	3416	3584	3409		
Relative	3553	3660	3439	3454	3373		
Nucleus accumbens							
Left							
Absolute	376	379	388	383	373	0.4	0.84
Relative	380	388	390	371	370	1.2	0.31
Right							
Absolute	370	366	373	378	369		
Relative	373	375	375	366	366		
Putamen							
Left							
Absolute	4767	4899	4868	4927	4692	1.2	0.33
Relative	4811	5022	4894	4775	4651	3.6	0.008*
Right							
Absolute	5074	5192	5137	5258	5020		
Relative	5119	5320	5165	5100	4977		
Globus pallidus							
Left							
Absolute	1648	1683	1615	1698	1589	1.9	0.11
Relative	1663	1726	1624	1646	1575	4.9	0.0009*
Right							
Absolute	1652	1687	1631	1711	1608		
Relative	1666	1728	1640	1661	1594		
Thalamus							
Left							
Absolute	7681	7495	7617	7751	7599	0.9	0.49
Relative	7749	7689	7658	7512	7533	1.9	0.12
Right							
Absolute	7353	7225	7289	7438	7237		
Relative	7412	7392	7325	7232	7181		

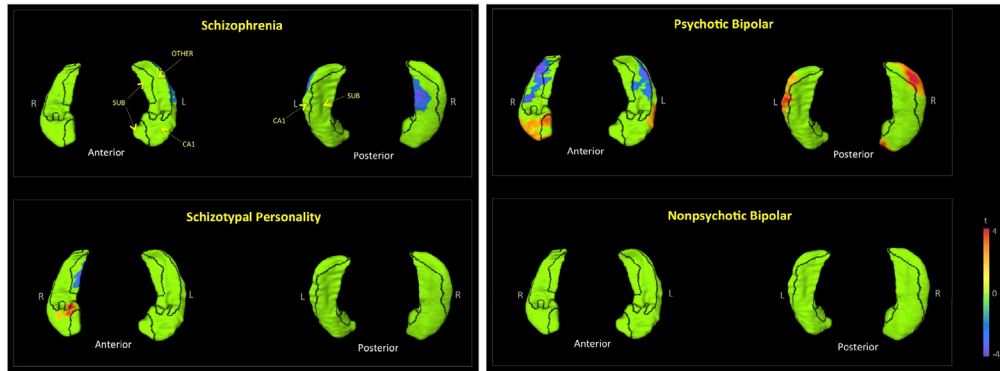
Reported volumes are in mm^3 .

All volumes and results were controlled for age and sex.

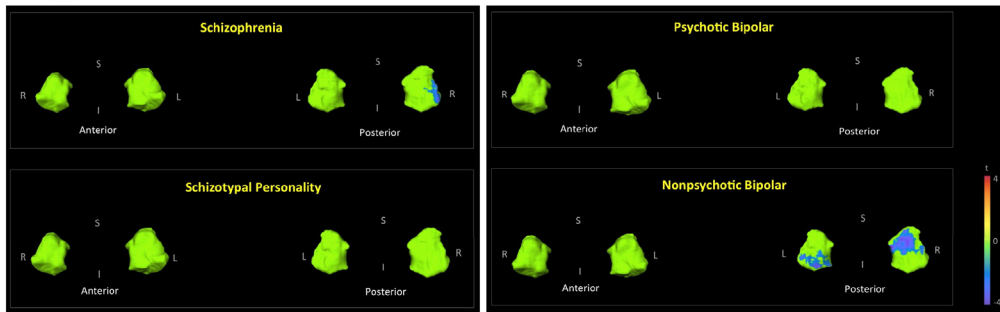
Results were derived from repeated measures ANOVA using hemisphere as a repeated measure.

* $p < 0.01$.

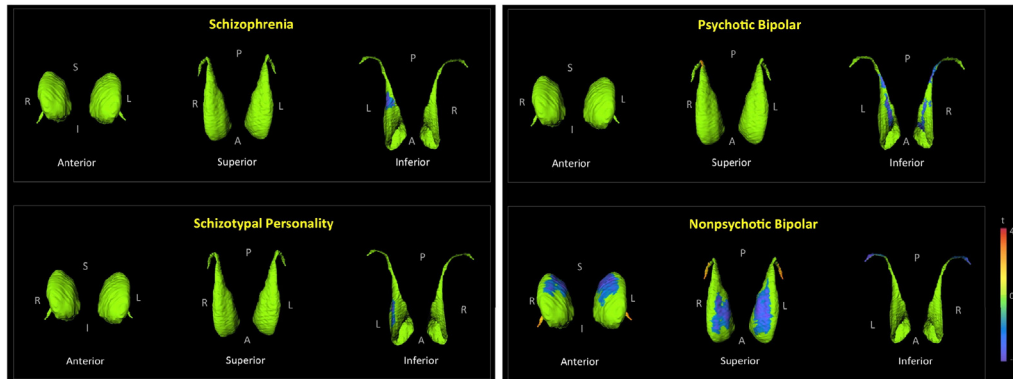
A. Hippocampus



B. Amygdala



C. Caudate



D. Nucleus Accumbens

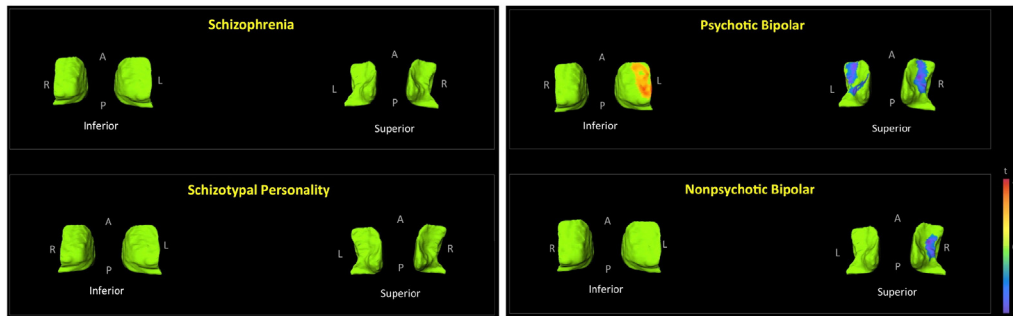
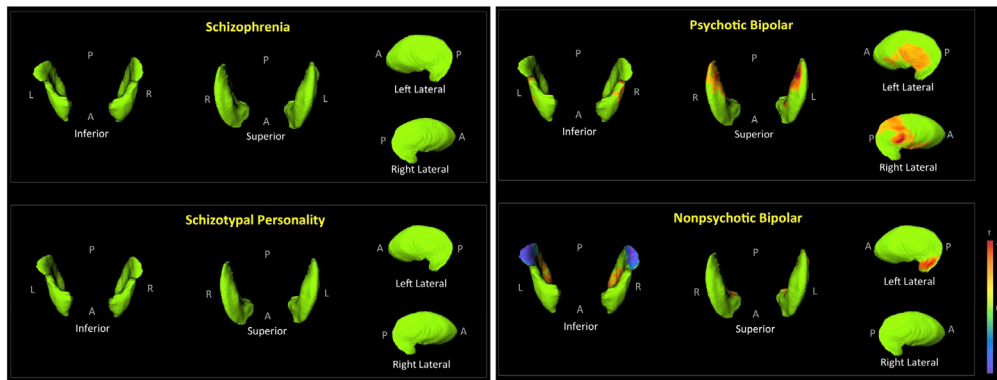
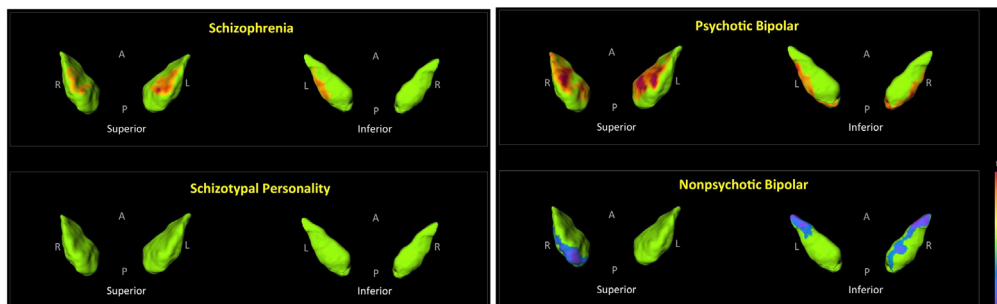


Fig. 1. Shape analysis of individual subcortical structures. The figures depict displacement maps, generated from mean surfaces of the indicated diagnostic groups relative to healthy controls, for the: hippocampus (A), amygdala (B), caudate (C), nucleus accumbens (D), putamen (E), globus pallidus (F), and thalamus (G). Results were corrected for age and sex. Demarcation lines on hippocampal and thalamic surfaces separate designated subfields or nuclei, and are indicated on the first listed comparisons. Hippocampal subfields: CA1, subiculum (SUB), and the remaining regions which include CA2, CA3, CA4 and the dentate gyrus (REM). Thalamic nuclei: anterior nucleus (ANT), medial dorsal nucleus (MD), pulvinar (PUL), and the remaining nuclei (REM), which include the lateral dorsal, lateral posterior, ventral anterior, ventral lateral, ventral intermedial, and ventral posterior nuclei, as well as the medial and lateral geniculate bodies. Regions in green did not show significant group differences after RFT multiple comparison correction. T-values with cooler colors ($t < 0$) indicate inward surface deformity, and warmer colors ($t > 0$) indicate outward surface deformity. (For interpretation of the references to color in this figure legend, the reader is referred to the web version of this article.)

E. Putamen



F. Globus Pallidus



G. Thalamus

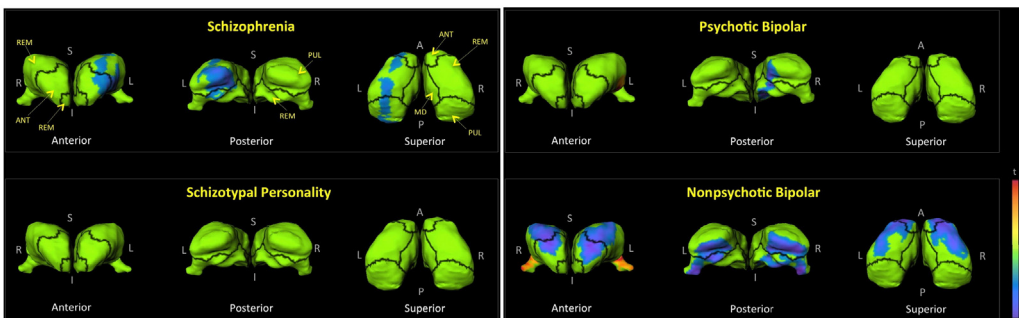


Fig. 1 (continued).

significant hemispheric effects for amygdala volume. Fig. 1B shows shape findings for the amygdala.

3.4. Caudate volume and shape

There were no significant group effects for caudate volume; and there were no significant hemispheric effects. Shape findings involving the caudate are shown in Fig. 1C. Including total intracranial volume as a covariate resulted in a significant group effect for caudate volume ($p = 0.001$). Post hoc analyses showed the following significant group effects for caudate volume on the left: CON > N-BP ($p = 0.018$); SCZ > SPE ($p = 0.012$); SCZ > P-BP ($p = 0.0007$); and SCZ > N-BP ($p = 0.0003$). Significant volume effects on the right were: CON > N-BP ($p = 0.029$); SCZ > SPE ($p = 0.04$); SCZ > P-BP ($p = 0.003$); and SCZ > N-BP ($p = 0.0005$). By correcting shape findings for intracranial size, we explored the regions of the caudate contributing to the described volumetric group differences. As seen in Fig. 2A, the increase in caudate volume in SCZ is localized to the most anterior region of the head.

3.5. Nucleus accumbens volume and shape

There were no significant group effects for nucleus accumbens volume (with or without intracranial volume correction). There were no significant hemispheric effects for volume. Fig. 1D shows shape findings for the nucleus accumbens.

3.6. Putamen volume and shape

There were no significant group effects for putamen volume. There were however significant hemispheric effects ($p < 0.0001$), but no group by hemisphere effects. Putamina were smaller on the left than on the right. Shape findings for the putamen are shown in Fig. 1E. Including total intracranial volume as a covariate resulted in a significant group effect for putamen volume ($p = 0.006$). Post hoc analyses showed the following significant group effects for volume on the left: CON < SCZ ($p = 0.01$); SCZ > P-BP ($p = 0.004$); and SCZ > N-BP ($p = 0.0003$). Significant effects for putamen volume on the right were: CON < SCZ ($p = 0.03$); SCZ > P-BP ($p = 0.02$); and SCZ > N-BP ($p = 0.002$). In SCZ, after correcting for intracranial volumes, surface

Table 3
Notable subcortical shape findings.

Surface Deformation	SCZ		STP		PBP		NPBP	
	L	R	L	R	L	R	L	R
Hippocampus								
Subiculum contraction	–	++	–	+	–	–	–	–
CA2–4 + dentate contraction	–	–	–	–	++	++	–	–
CA1 contraction	+	–	–	–	–	–	–	–
CA1 expansion	–	–	+	+	++	++	–	–
Amygdala								
Posteriolateral contraction	–	+	–	–	–	–	–	–
Posteromedial contraction	–	–	–	–	–	–	+	++
Caudate								
Ventral contraction	+	–	+	–	+	+	–	–
Dorsal contraction	–	–	–	–	–	–	++	++
Nucleus Accumbens								
Ventral contraction	–	–	–	–	+	+	–	+
Dorsolateral expansion	–	–	–	–	+	–	–	–
Putamen								
Posteromedial contraction	–	–	–	–	–	–	+	+
Posterolateral expansion	–	–	–	–	–	–	+	–
Mediolateral expansion	–	–	–	–	+	+	–	–
Medial expansion	–	–	–	–	–	–	+	+
Posterosuperior expansion	–	–	–	–	+	+	–	–
Globus pallidus								
Anterosuperior contraction	–	–	–	–	–	–	–	+
Inferior contraction	–	–	–	–	–	–	+	+
Superomedial expansion	+	+	–	–	++	++	–	–
Lateral expansion	+	–	–	–	+	+	–	–
Thalamus								
Anterior contraction	+	–	–	–	–	–	++	++
Pulvinar contraction	+	–	–	–	–	+	++	++
Superior contraction	+	–	–	–	–	–	++	++

Surface deformation estimates are derived from comparisons of mean groups to mean control subjects, and controlled for age and sex.

+ : mild or moderate surface deformation.

++ : large surface deformation.

expansion was observed in the posterior dorsal putamen, and laterally on the right (Fig. 2A). No surface expansion was seen in the other groups (Fig. 2B–D).

3.7. Globus pallidus volume and shape

There were no significant group effects or hemispheric effects for globus pallidus volume. Shape findings are shown in Fig. 1F. Including total intracranial volume as a covariate resulted in a significant group effect for volume ($p = 0.0007$). Post hoc analyses showed the following significant group volume effects on the left: CON < SCZ ($p = 0.02$); CON > N-BP ($p = 0.009$); SCZ > SPE ($p = 0.02$); SCZ > P-BP ($p = 0.004$); SCZ > N-BP ($p < 0.0001$); and P-BP > N-BP ($p = 0.03$). Significant volume effects on the right were: CON < SCZ ($p = 0.03$); CON > N-BP ($p = 0.04$); SCZ > P-BP ($p = 0.02$); and SCZ > N-BP ($p = 0.0002$). Fig. 2A shows surface deformation in SCZ after correcting for intracranial volumes. Regions of surface expansion were present dorsally along the ventrolateral edges.

3.8. Thalamus volume and shape

There were no significant group volume effects, and correcting for intracranial volumes did not change overall results. There were also no significant hemispheric effects for volume. Shape findings involving the thalamus are shown in Fig. 1G.

3.9. Clinical correlations

Correlation results are shown in Table 4. Total gray matter volume inversely correlated with total SANS ($r = -0.25$; $p = 0.0009$) and SAPS positive symptoms ($r = -0.2$; $p = 0.008$), but not with SAPS disorganization symptoms. Cortical white matter volume showed a significant inverse relationship with the SANS ($r = -0.16$; $p = 0.03$), but not

with SAPS domains. Among the subcortical structures, significant clinical relationships were only found for the hippocampus, amygdala and thalamus. The left hippocampus only correlated with SAPS disorganization ($r = -0.19$; $p = 0.01$) and SANS ($r = -0.21$; $p = 0.006$). There were no significant correlations for the right hippocampus. Both left and right amygdala volumes were significantly related to SANS scores (left: $r = -0.17$, $p = 0.02$; right: $r = -0.19$, $p = 0.01$). Similarly, both left and right thalamus volumes were significantly related to SANS scores (left: $r = -0.16$, $p = 0.03$; right: $r = -0.15$, $p = 0.049$).

In those subcortical structures with group volume differences, vertex deformation was also investigated relative to clinical domain scores, excluding diagnosis, age and sex effects (Fig. 3). Hippocampal contraction with disorganization and negative symptoms was localized mainly to the lateral CA1 region. Additionally, negative symptoms were related to medial subiculum contraction. Positive symptoms, on the other hand were associated with anterior CA1 contraction (Fig. 3A). Reduced volumes of the amygdala with negative symptoms involved diffuse surface regions, most notably on the right posterior surface (Fig. 3B). Thalamus volume contraction with negative symptoms was localized to the lateral thalamic surface; while that with positive symptoms was mainly localized to the anterior and posterior extremes.

4. Discussion

Shape analysis complements volumetric analysis, and can identify subtle regional abnormalities on brain structures helping to localize specific pathophysiologic pathways. Our study compared the volumes and shapes of multiple subcortical brain structures in healthy and psychiatric populations. We did not find absolute volumetric group differences for any of the subcortical structures studied, but some structures showed differences after controlling for brain size. Shape analysis on the other hand showed regional surface deformations in each diagnostic group. Contrary to our expectation, we only found little overlap in the pattern of deformation across groups.

4.1. Hippocampus

In our study, hippocampal shape analyses revealed regional group differences despite similar volumes across groups. In SCZ, the hippocampus was most deformed on the right side with shrinkage in the ventral subiculum. The subiculum receives input from CA1 and entorhinal cortical layer III pyramidal neurons and is the main output of the hippocampus (Small et al., 2011). Given the widespread set of cortical and subcortical areas with which it interacts, it is able to influence activity in disparate brain regions (Small et al., 2011; O'Mara, 2005). Although the exact roles of the subiculum are unclear, it has been suggested that there is a segregation of function within the subiculum: the dorsal component mainly being involved in processing of spatial, movement and memory information; and the ventral component playing a major role in the inhibition of the HPA axis stress response (O'Mara, 2005). Smaller hippocampi is often seen in studies of SCZ patients (Shepherd et al., 2012; Adriano et al., 2012) as well as smaller subiculum volumes (Haukvik et al., 2015). Results regarding the location of hippocampal shrinkage however have varied across studies, having been reported in the head or anterior region (Csernansky et al., 2002; Mamah et al., 2012; Johnson et al., 2013; Qiu et al., 2010; Zierhut et al., 2013) and the body or tail (Liberg et al., 2014; Liberg et al., 2015). Furthermore, CA1 regional deformation has been described in SCZ (Csernansky et al., 2002; Small et al., 2011). We found that in STP participants, the hippocampus was less deformed than in SCZ, without any notable overlapping regions. However, similar to SCZ, the STP group had hippocampal deformations in the subiculum, which thus may indicate a role of this region in schizophrenia spectrum disorder neurobiology. In the P-BP participants, hippocampal shrinkage involved regions outside of the subiculum and CA1; however N-BP participants had normal hippocampi suggesting that psychosis status in BP may be associated with

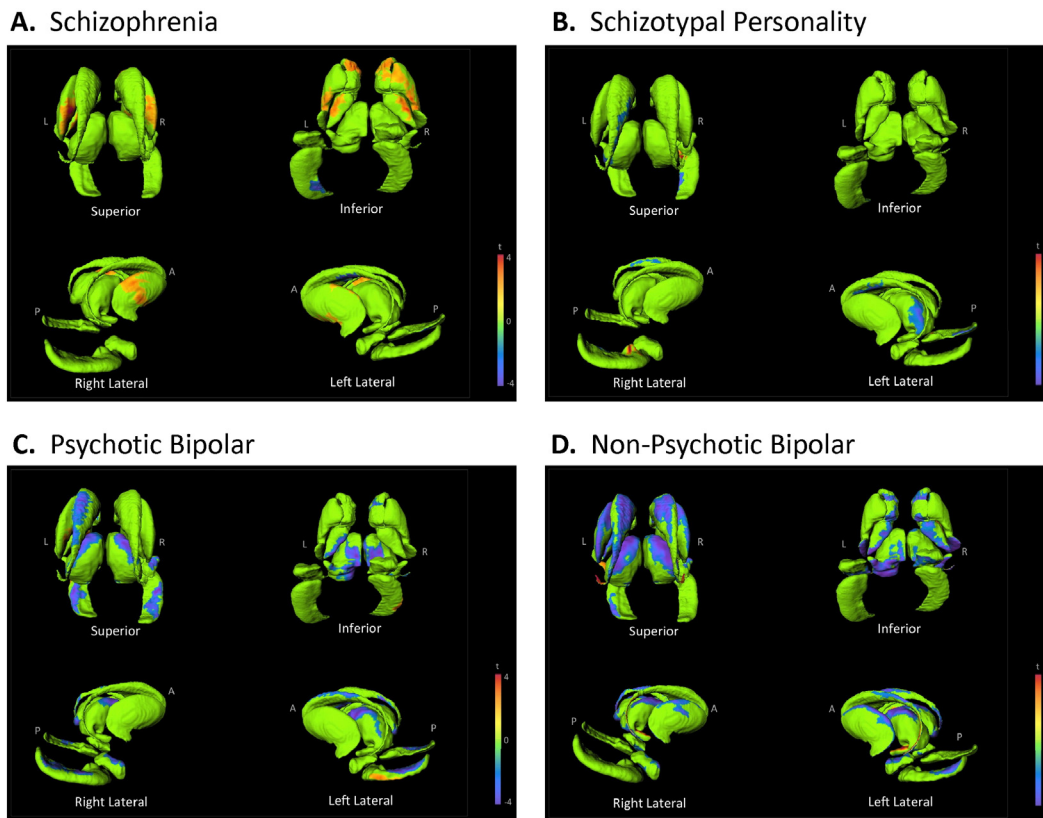


Fig. 2. Shape analysis after brain size correction. The figures depict displacement maps for the basal ganglia (i.e. caudate, nucleus accumbens, putamen, and globus pallidus) and thalamus, presented together as they appear naturally. Maps were generated from mean surfaces of the indicated diagnostic groups relative to healthy controls. Results were corrected for age, sex and intracranial volume. Regions in green did not show significant group differences after RFT multiple comparison correction. T-values with cooler colors ($t < 0$) indicate inward surface deformity, and warmer colors ($t > 0$) indicate outward surface deformity. A = anterior; P = posterior; L = left; R = right.

hippocampal deformation. Smaller hippocampi are seen less commonly in BP than in SCZ (Otten and Meeter, 2015; van Erp et al., 2012). Shrinkage of the head and medial border of the left hippocampus has been reported in BP, along with expansion on the right hippocampal tail medially (Quigley et al., 2015). Our study results also showed a relationship between clinical symptoms and smaller hippocampal volumes on the left side. While our study did not show significant volumetric group effects, there was a trend level effect for left hippocampal volume in SCZ. This is consistent with some studies that have found a reduction in hippocampal size selectively on the left side (Kawano et al., 2015; Stefanis et al., 1999). Smaller left hippocampus has also been found to be a risk indicator for psychosis (Seidman et al., 2002) and may indicate a preferential vulnerability of the left hippocampus to environmental stress (Stefanis et al., 1999; Mohanakrishnan Menon et al., 2003; Shu et al., 2013).

4.2. Amygdala

Few studies have evaluated amygdala shape in psychiatric disorders. Surface deflation of the left amygdala has been reported in first episode mania and bilaterally in first episode SCZ (Qiu et al., 2013). Others found bilateral shrinkage of the basolateral, basomedial and centromedial amygdala and the left lateral subregion in SCZ compared to P-BP (Mahon et al., 2015). Negative findings have also been reported in SCZ (Shenton et al., 2002). In our study, we found that the amygdala in SCZ has several shrunken regions, principally those corresponding to lateral and centromedial subfields. Both BP subgroups showed more extensive shrinkage than SCZ. Regional deformation may be relevant to abnormal emotional processing, particularly in BP patients. Sensory inputs to the amygdala (e.g. from the hippocampus, primary auditory cortex, processed visual information from temporal cortex)

terminate in the lateral nucleus. The structural organization and cellular composition of the lateral portions of the amygdala are cortex-like, and the majority of neurons are glutamatergic projection neurons. In contrast, the medial structures are striatum-like, and consist of GABAergic neurons (Lee et al., 2013; Ehrlich et al., 2009). Our findings therefore suggest structural abnormalities involving both excitatory and inhibitory neurons of the amygdala in SCZ and BP.

4.3. Thalamus

In the SCZ thalamus, we observed surface contraction in the pulvinar and ventral lateral nucleus. The pulvinar is a collection of nuclei with widespread connections to areas that include visual cortex, posterior parietal cortex, cingulate, premotor, prefrontal and the superior colliculi (Grieve et al., 2000) and is involved in visual attention including linking visual stimuli with context-specific motor responses (Grieve et al., 2000; Arend et al., 2008). In addition to visual salience, the pulvinar also has been implicated in social cognition, including face processing (Benarroch, 2015; Nguyen et al., 2013; Saalman and Kastner, 2013). The ventral lateral nucleus targets efferents including the motor cortex, premotor cortex and supplementary motor cortex, facilitating the coordination and planning of movement. Previous shape studies in SCZ have found decreased sizes of various nuclei including the pulvinar, and the ventral lateral, anterior and mediodorsal nuclei (Csernansky et al., 2004; Smith et al., 2011; Danivas et al., 2013). In the current study, the BP participants also showed posterior thalamic shrinkage. However, BP participants also had shrinkage in regions of the anterior and dorsal lateral nuclei. Connectionally and structurally, the lateral dorsal nuclei are reportedly similar to that of the anterior nuclei, and play a role in spatial memory and learning (van Groen et al., 2002). The clinical relevance of the observed shape abnormalities is

Table 4
Clinical correlations.

Region	Positive symptoms ^a	Disorg. symptoms ^b	Negative symptoms ^c	p ^a	p ^b	p ^c
Total gray matter	−0.20	−0.13	−0.25	0.008*	0.08	−0.0009*
Cortical white matter	−0.09	−0.05	−0.16	0.24	0.37	0.03*
Hippocampus						
Left	−0.14	−0.19	−0.21	0.06	0.01	0.006
Right	−0.10	−0.12	0.14	0.17	0.12	0.06
Amygdala						
Left	−0.08	−0.13	−0.17	0.28	0.09	0.02*
Right	−0.09	−0.13	−0.19	0.21	0.08	0.01*
Caudate						
Left	−0.05	−0.11	−0.09	0.49	0.15	0.24
Right	−0.07	−0.13	−0.08	0.39	0.09	0.28
Nucleus accumbens						
Left	−0.13	−0.02	−0.06	0.09	0.75	0.42
Right	−0.14	−0.02	−0.09	0.07	0.77	0.26
Putamen						
Left	−0.06	−0.06	−0.02	0.45	0.43	0.81
Right	−0.08	−0.06	−0.03	0.32	0.33	0.67
Globus pallidus						
Left	0.00	−0.02	−0.05	0.99	0.83	0.51
Right	−0.03	−0.01	−0.04	0.67	0.82	0.63
Thalamus						
Left	−0.15	−0.07	−0.16	0.04*	0.36	0.03*
Right	−0.14	−0.05	−0.15	0.07	0.55	0.05*

Relationships were analyzed using Pearson correlations partially controlled for diagnosis, age and sex.

^a relates to positive symptoms (derived from SAPS) Pearson's r or p values.

^b relates to disorganized symptoms (derived from SAPS) Pearson's r or p values.

^c relates to negative symptoms (derived from SANS) Pearson's r or p values.

* p < 0.05.

suggested by results of our correlational analyses, which showed that psychotic symptoms were localized to anterior and posterior thalamic nuclei.

4.4. Basal ganglia

Brain size corrected analyses resulted in significant group volume effects in the basal ganglia, driven primarily by enlargement in SCZ. Basal ganglia enlargement was localized to specific surface regions (across all nuclei), generally with some symmetry. The significance of the affected regions is unclear, and do not correlate with the distribution dopaminergic receptor subtypes (Rosa-Neto et al., 2004). Considering the well documented medication effects on basal ganglia structures (Mamah et al., 2007; Breier et al., 1992; McCarley et al., 1999; Staal et al., 2000; van Erp et al., 2016), it is probable that basal ganglia enlargement in our study is a consequence of past use of typical antipsychotic drugs (such as haloperidol or fluphenazine), which are predominantly antagonists of the D₂-subtype dopaminergic receptor. These receptors are highly abundant in the striatum, which have substantial dopaminergic afferents from the substantia nigra and the ventral tegmental area (Rosa-Neto et al., 2004; Hall et al., 1994). In animal studies, D₂-receptor blockade has been shown to cause striatal enlargement in multiple studies (Chakos et al., 1998; Andersson et al., 2002; Vernon et al., 2012). Most other investigators have also observed volume enlargement of basal ganglia nuclei in SCZ patients (Mamah et al., 2007; Breier et al., 1992; McCarley et al., 1999; Staal et al., 2000; van Erp et al., 2016). A positive correlation between typical antipsychotic dose and striatal volume has been observed, supporting a trophic effect (Chakos et al., 1994; DeLisi et al., 1991; Doraiswamy et al., 1995; Gur et al., 1998; Shihabuddin et al., 1998; Swayze et al., 1992). In contrast to volume increases with typical antipsychotics, normal (Gunduz et al., 2002) and decreased (Corson et al., 1999; Keshavan et al., 1998) basal ganglia volumes are generally reported in neuroleptic-naïve

patients or those on newer generation antipsychotic drugs. Also, an absence of basal ganglia enlargement in unaffected schizophrenia relatives is typical (Mamah et al., 2008; Staal et al., 2000) although some authors have found increased basal ganglia size in relatives (Oertel-Knochel et al., 2012). Several mechanisms underlying basal ganglia volume increase following D₂-receptor blockade have been proposed. Disruption of the normal homeostatic mechanisms of target neurons in the basal ganglia appears to occur leading to a number of compensatory changes, manifesting as hypertrophy macroscopically (Andersson et al., 2002; Konradi and Heckers, 2001). Chronic haloperidol use has been associated with increased synaptic density in the striatum, (Meshul and Casey, 1989; Meshul et al., 1994; Eastwood et al., 1997) mainly of the glutamatergic type (Meshul and Casey, 1989; Kerns et al., 1992; See et al., 1992; Uranova et al., 1991) and possibly associated with increased synaptophysin expression (Eastwood et al., 1997). Others have found increased neuronal size, particularly in axon terminals in the striatum, (Kerns et al., 1992; Uranova et al., 1991; Benes et al., 1985) or an increase in the number of striatal neurons (Beckmann and Lauer, 1997; Lauer and Beckmann, 1997). Complicating the understanding of antipsychotic trophic effects is that long-term treatment or high dosing can also induce neurotoxicity and loss of brain volume (Andreassen and Jorgensen, 2000; Burkhardt et al., 1993; Goff et al., 1995; Altunkaynak et al., 2012). Therefore, dependent on drug concentration, treatment time and individual sensitivity, the neurotrophic or neurotoxic properties appear to determine basal ganglia volume increase or decrease respectively (Konradi and Heckers, 2001). By contrast to SCZ, both BP subgroups had multiple deflated regions, presumably since typical antipsychotics are infrequently used in these populations. This is particularly true for N-BP patients, who had the most extensive basal ganglia deflation. Basal ganglia surface deflation has been previously reported in BP, with variable findings: in the anterior and ventral striatum, (Hwang et al., 2006) dorsal caudate, (Womer et al., 2014) left ventromedial caudate (Ong et al., 2012) and right putamen (Liberg et al., 2014). Others found no surface abnormality in BP, but a relationship of striatal deflation to illness severity (Liberg et al., 2015).

4.5. Conclusions & limitations

In summary, our study found group differences in surface shapes of several subcortical brain structures, despite an absence of volumetric effects. Surface deformation patterns in individual diagnostic groups were largely unique; however related deformities were seen in the posterior thalamus in SCZ, P-BP and N-BP, as well as in the hippocampal subiculum in SCZ and STP. Basal ganglia surface enlargements in SCZ suggested typical antipsychotic drug effects. The results of our studies suggest distinct neurobiological abnormalities in each disorder, with minimal overlap across disorders. Findings however can be confounded by factors, which can limit the conclusion drawn from our study. Medications and recreational drugs could also influence brain structure (other than the basal ganglia), which are difficult to correct. For example, the typical antipsychotic drug, haloperidol has been reported to decrease cortical gray matter and whole brain volume, (Vernon et al., 2012) as well as subcortical structures such as the hippocampus (Mamah et al., 2012). Lithium and antidepressant drugs have also been reported to increase cortical gray matter (Otten and Meeter, 2015; Vernon et al., 2012; Hajek et al., 2014; Connor et al., 2004; Hartberg et al., 2015). However, studies showing similar regional deformations in nonpsychotic and unmedicated siblings of patients suggest that surface structural abnormalities can be fairly well estimated despite potential drug effects (Mamah et al., 2008; Harms et al., 2007; Tepest et al., 2003). The FS + LDDMM shape methodology, while robust, may also be less accurate in delineating smaller structures (Khan et al., 2008). Thus, results may have underestimated shape abnormalities in the smaller nucleus accumbens or amygdala. Future studies involving more extensive behavioral measures, including cognition, would also be beneficial in further clarifying the clinical relationships of regional

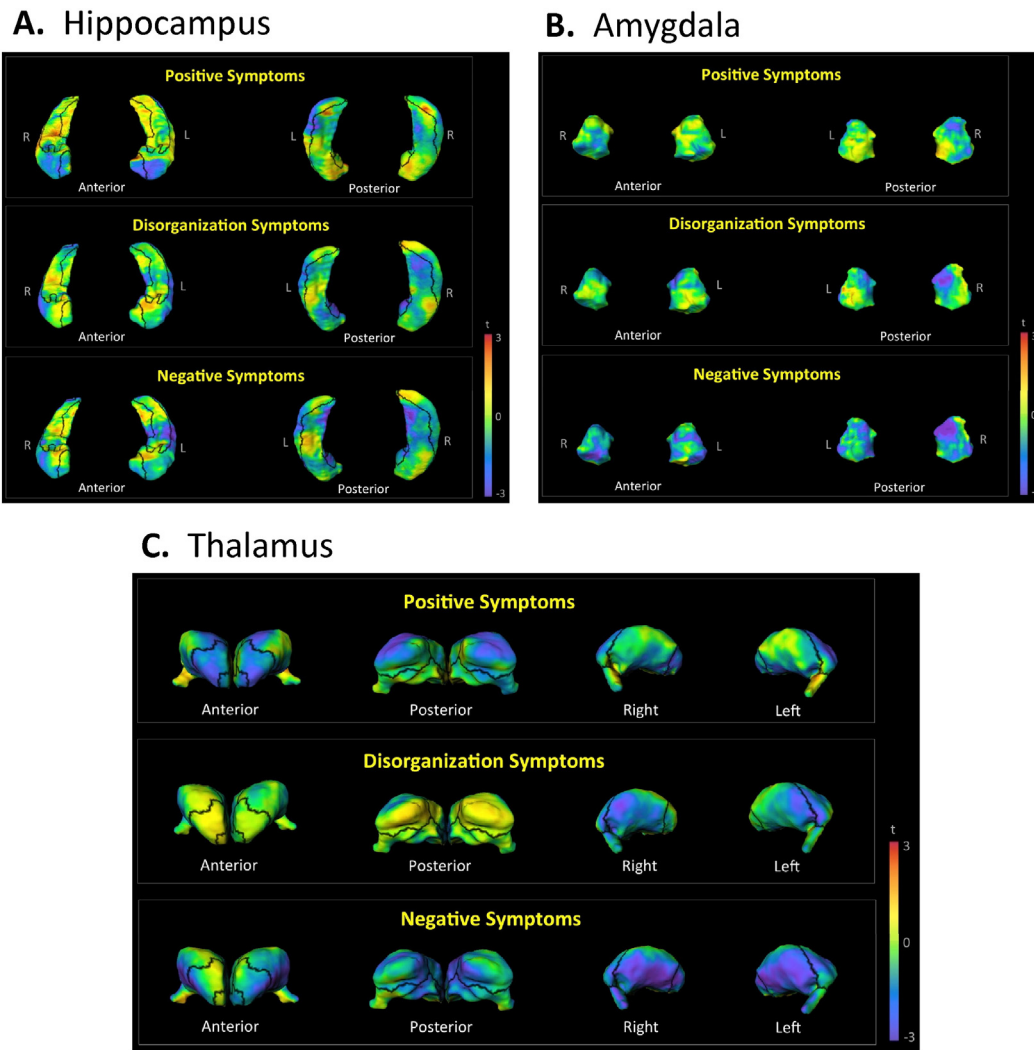


Fig. 3. Shape relationships to clinical symptoms. The maps show regression coefficients for the hippocampus, amygdala, and thalamus against the positive, disorganized or negative symptoms. Cooler colors indicate inward surface deformity, and warmer colors indicate outward surface deformity.

surface deformations. Developments in morphometric methods may allow more precise early identification of psychiatric disorders and risk states, and aid the monitoring of treatment effects.

Acknowledgements

This research was supported by NIH grants P50 MH071616, R01 MH56584 and K08 MH085948. Dr. Mamah has received grants from the NIMH (MH085948), NARSAD, the McDonnell Center for Systems Neuroscience, the Taylor Family Institute and Eli Lilly. Dr. Barch has received grants from the NIMH (MH071616, MH56584), NIA, NARSAD, and Allon, Novartis, and the McDonnell Center for Systems Neuroscience and has consulted for Pfizer. Dr. Csernansky was a consultant to Lundbeck Pharmaceuticals in the last year. Other authors have no biomedical financial interests or potential conflicts of interest to declare.

References

- Adler, R.J., 1981. *The Geometry of Random Fields*. Wiley, New York.
- Adler, R.J., Hasofer, A.M., 1976. Level-crossings for random fields. *Ann. Probab.* 4 (1), 1–12.
- Adriano, F., Caltagirone, C., Spalletta, G., 2012. Hippocampal volume reduction in first-episode and chronic schizophrenia: a review and meta-analysis. *Neuroscientist* 18 (2), 180–200 Apr.
- Altunkaynak, B.Z., Ozbek, E., Unal, B., Aydin, N., Aydin, M.D., Vuraler, O., 2012. Chronic treatment of haloperidol induces pathological changes in striatal neurons of guinea pigs: a light and electron microscopical study. *Drug Chem. Toxicol.* 35 (4), 406–411 Oct.
- Andersson, C., Hamer, R.M., Lawler, C.P., Mailman, R.B., Lieberman, J.A., 2002. Striatal volume changes in the rat following long-term administration of typical and atypical antipsychotic drugs. *Neuropsychopharmacology* 27 (2), 143–151 Aug.
- Andreasen, N.C., Arndt, S., Alliger, R., Miller, D., Flaum, M., 1995. Symptoms of schizophrenia: methods, meanings, and mechanisms. *Arch. Gen. Psychiatry* 52, 341–351.
- Andreassen, O.A., Jorgensen, H.A., 2000. Neurotoxicity associated with neuroleptic-induced oral dyskinesias in rats. Implications for tardive dyskinesia? *Prog. Neurobiol.* 61 (5), 525–541 Aug.
- Arend, I., Machado, L., Ward, R., McGrath, M., Ro, T., Rafal, R.D., 2008. The role of the human pulvinar in visual attention and action: evidence from temporal-order judgment, saccade decision, and antisaccade tasks. *Prog. Brain Res.* 171, 475–483.
- Ballmaier, M., Schlagenhaut, F., Toga, A.W., et al., 2008. Regional patterns and clinical correlates of basal ganglia morphology in non-medicated schizophrenia. *Schizophr. Res.* 106 (2–3), 140–147 Dec.
- Beckmann, H., Lauer, M., 1997. The human striatum in schizophrenia. II. Increased number of striatal neurons in schizophrenics. *Psychiatry Res.* 68 (2–3), 99–109 Feb 7.
- Beg, M.F., Miller, M.J., Trounev, A., Younes, L., 2005. Computing large deformation metric mappings via geodesic flows of diffeomorphisms. *Int. J. Comput. Vis.* 61, 139–157.
- Benarroch, E.E., 2015. Pulvinar Associative role in cortical function and clinical correlations. *Neurology* 84 (7), 738–747 Feb 17.
- Benes, F.M., Paskevich, P.A., Davidson, J., Domesick, V.B., 1985. The effects of haloperidol on synaptic patterns in the rat striatum. *Brain Res.* 329 (1–2), 265–273 Mar 11.
- Breier, A., Buchanan, R.W., Elkashef, A., Munson, R.C., Kirkpatrick, B., Gellad, F., 1992. Brain morphology and schizophrenia. A magnetic resonance imaging study of limbic, prefrontal cortex, and caudate structures. *Arch. Gen. Psychiatry* 49 (12), 921–926 Dec.
- Burkhardt, C., Kelly, J.P., Lim, Y.H., Filley, C.M., Parker Jr., W.D., 1993. Neuroleptic medications inhibit complex I of the electron transport chain. *Ann. Neurol.* 33 (5), 512–517 May.
- Cardno, A.G., Owen, M.J., 2014. Genetic relationships between schizophrenia, bipolar disorder, and schizoaffective disorder. *Schizophr. Bull.* 40 (3), 504–515 May.
- Ceyhan, E., Beg, M.F., Ceritoglu, C., et al., 2011. Quantization and analysis of hippocampal morphometric changes due to dementia of Alzheimer type using metric distances

- based on large deformation diffeomorphic metric mapping. *Comput. Med. Imaging Graph* 35 (4), 275–293 Jun.
- Chakos, M.H., Lieberman, J.A., Bilder, R.M., et al., 1994. Increase in caudate nuclei volumes of first-episode schizophrenic patients taking antipsychotic drugs. *Am. J. Psychiatry* 151 (10), 1430–1436 Oct.
- Chakos, M.H., Shirakawa, O., Lieberman, J., Lee, H., Bilder, R., Tamminga, C.A., 1998. Striatal enlargement in rats chronically treated with neuroleptic. *Biol. Psychiatry* 44 (8), 675–684 Oct 15.
- Chumbley, J.R., Friston, K.J., 2009. False discovery rate revisited: FDR and topological inference using Gaussian random fields. *NeuroImage* 44 (1), 62–70 Jan 1.
- Chung, M.K., Worsley, K.J., Nacewicz, B.M., Dalton, K.M., Davidson, R.J., 2010. General multivariate linear modeling of surface shapes using SurfStat. *Neuroimage* 53 (2), 491–505 Nov 1.
- Connor, S.E., Ng, V., McDonald, C., et al., 2004. A study of hippocampal shape anomaly in schizophrenia and in families multiply affected by schizophrenia or bipolar disorder. *Neuroradiology* 46 (7), 523–534 Jul.
- Corson, P.W., Nopoulos, P., Andreasen, N.C., Heckel, D., Arndt, S., 1999. Caudate size in first-episode neuroleptic-naive schizophrenic patients measured using an artificial neural network. *Biological Psychiatry* 46 (5), 712–720 Sep 1.
- Csernansky, J.G., Wang, L., Jones, D., et al., 2002. Hippocampal deformities in schizophrenia characterized by high dimensional brain mapping. *Am. J. Psychiatry* 159 (12), 2000–2006 Dec.
- Csernansky, J.G., Schindler, M.K., Splinter, N.R., et al., 2004. Abnormalities of thalamic volume and shape in schizophrenia. *Am. J. Psychiatry* 161 (5), 896–902 May.
- Danivas, V., Kalmady, S.V., Venkatasubramanian, G., Gangadhar, B.N., 2013. Thalamic shape abnormalities in antipsychotic naive schizophrenia. *Indian J. Psychol. Med.* 35 (1), 34–38 Jan.
- DeLisi, L.E., Hoff, A.L., Schwartz, J.E., et al., 1991. Brain morphology in first-episode schizophrenic-like psychotic patients: a quantitative magnetic resonance imaging study. *Biol. Psychiatry* 29 (2), 159–175 Jan 15.
- Desikan, R.S., Segonne, F., Fischl, B., et al., 2006. An automated labeling system for subdividing the human cerebral cortex on MRI scans into gyral based regions of interest. *Neuroimage* 31 (3), 968–980 Jul 1.
- Doraiswamy, P.M., Tupler, L.A., Krishnan, K.R., 1995. Neuroleptic treatment and caudate plasticity. *Lancet* 345 (8951), 734–735 Mar 18.
- Draganski, B., Kherif, F., Klöppel, S., et al., 2008. Evidence for segregated and integrative connectivity patterns in the human Basal Ganglia. *J. Neurosci. Off. J. Soc. Neurosci.* 28 (28), 7143–7152 Jul 9.
- Eastwood, S.L., Heffernan, J., Harrison, P.J., 1997. Chronic haloperidol treatment differentially affects the expression of synaptic and neuronal plasticity-associated genes. *Mol. Psychiatry* 2 (4), 322–329 Jul.
- Ehrlich, I., Humeau, Y., Grenier, F., Ciocchi, S., Herry, C., Luthi, A., 2009. Amygdala inhibitory circuits and the control of fear memory. *Neuron* 62 (6), 757–771 Jun 25.
- Genovese, C.R., Lazar, N.A., Nichols, T., 2002. Thresholding of statistical maps in functional neuroimaging using the false discovery rate. *NeuroImage* 15 (4), 870–878 April.
- Goff, D.C., Tsai, G., Beal, M.F., Coyle, J.T., 1995. Tardive dyskinesia and substrates of energy metabolism in CSF. *Am. J. Psychiatry* 152 (12), 1730–1736 Dec.
- Grieve, K.L., Acuna, C., Cudeiro, J., 2000. The primate pulvinar nuclei: vision and action. *Trends Neurosci.* 23 (1), 35–39 Jan.
- Gunduz, H., Wu, H., Ashtari, M., et al., 2002. Basal ganglia volumes in first-episode schizophrenia and healthy comparison subjects. *Biol. Psychiatry* 51 (10), 801–808 May 15.
- Gur, R.E., Maany, V., Mozley, P.D., Swanson, C., Bilker, W., Gur, R.C., 1998. Subcortical MRI volumes in neuroleptic-naive and treated patients with schizophrenia. *Am. J. Psychiatry* 155 (12), 1711–1717 Dec.
- Hajek, T., Bauer, M., Simhandl, C., et al., 2014. Neuroprotective effect of lithium on hippocampal volumes in bipolar disorder independent of long-term treatment response. *Psychol. Med.* 44 (3), 507–517 Feb.
- Hall, H., Sedvall, G., Magnusson, O., Kopp, J., Halldin, C., Farde, L., 1994. Distribution of D1- and D2-dopamine receptors, and dopamine and its metabolites in the human brain. *Neuropsychopharmacology* 11 (4), 245–256 Dec.
- Harms, M.P., Wang, L., Mamah, D., Barch, D.M., Thompson, P.A., Csernansky, J.G., 2007. Thalamic shape abnormalities in individuals with schizophrenia and their nonpsychotic siblings. *J. Neurosci.* 27 (50), 13835–13842 Dec 12.
- Hartberg, C.B., Jorgensen, K.N., Haukvik, U.K., et al., 2015. Lithium treatment and hippocampal subfields and amygdala volumes in bipolar disorder. *Bipolar Disord.* 17 (5), 496–506 Aug.
- Haukvik, U.K., Westlye, L.T., Mørch-Johnsen, L., et al., 2015. In vivo hippocampal subfield volumes in schizophrenia and bipolar disorder. *Biol. Psychiatry* 77 (6), 581–588 Mar 15.
- Hwang, J., Lyoo, I.K., Dager, S.R., et al., 2006. Basal ganglia shape alterations in bipolar disorder. *Am. J. Psychiatry* 163 (2), 276–285 Feb.
- Johnson, S.L., Wang, L., Alpert, K.I., et al., 2013. Hippocampal shape abnormalities of patients with childhood-onset schizophrenia and their unaffected siblings. *J. Am. Acad. Child Adolesc. Psychiatry* 52 (5), 527–536 May. (e522).
- Kang, D.H., Kim, S.H., Kim, C.W., et al., 2008. Thalamus surface shape deformity in obsessive-compulsive disorder and schizophrenia. *Neuroreport* 19 (6), 609–613 Apr 16.
- Kawano, M., Sawada, K., Shimodera, S., et al., 2015. Hippocampal subfield volumes in first episode and chronic schizophrenia. *PLoS ONE* 10 (2), e0117785.
- Kerns, J.M., Sierens, D.K., Kao, L.C., Klawans, H.L., Carvey, P.M., 1992. Synaptic plasticity in the rat striatum following chronic haloperidol treatment. *Clin. Neuropharmacol.* 15 (6), 488–500 Dec.
- Keshavan, M.S., Rosenberg, D., Sweeney, J.A., Pettegrew, J.W., 1998. Decreased caudate volume in neuroleptic-naive psychotic patients. *Am. J. Psychiatry* 155 (6), 774–778 Jun.
- Khan, A.R., Wang, L., Beg, M.F., 2008. FreeSurfer-initiated fully-automated subcortical brain segmentation in MRI using Large Deformation Diffeomorphic Metric Mapping. *Neuroimage* 41 (3), 735–746 Jul 1.
- Konradi, C., Heckers, S., 2001. Antipsychotic drugs and neuroplasticity: insights into the treatment and neurobiology of schizophrenia. *Biol. Psychiatry* 50 (10), 729–742 Nov 15.
- Lauer, M., Beckmann, H., 1997. The human striatum in schizophrenia. I. Increase in overall relative striatal volume in schizophrenics. *Psychiatry Res.* 68 (2–3), 87–98 Feb 7.
- Lee, S., Kim, S.J., Kwon, O.B., Lee, J.H., Kim, J.H., 2013. Inhibitory networks of the amygdala for emotional memory. *Front. Neural Circuits* 7, 129.
- Lehericy, S., Ducros, M., Van de Moortele, P.F., et al., 2004. Diffusion tensor fiber tracking shows distinct corticostriatal circuits in humans. *Ann. Neurol.* 55 (4), 522–529 Apr.
- Levitt, J.J., Westin, C.F., Nestor, P.G., et al., 2004. Shape of caudate nucleus and its cognitive correlates in neuroleptiR-GO-Rég várok valakire(koncert felvétel) - Duration: 4:29. Öcsi Nagy 44,785 viewsw-naive schizotypal personality disorder. *Biol. Psychiatry* 55 (2), 177–184 Jan 15.
- Levitt, J.J., Styner, M., Niethammer, M., et al., 2009. Shape abnormalities of caudate nucleus in schizotypal personality disorder. *Schizophr. Res.* 110 (1–3), 127–139 May.
- Liberg, B., Ekman, C.J., Sellgren, C., Johansson, A., Landen, M., 2014. Vertex-based morphometry in euthymic bipolar disorder implicates striatal regions involved in psychomotor function. *Psychiatry Res.* 221 (3), 173–178 Mar 30.
- Liberg, B., Ekman, C.J., Sellgren, C., Johansson, A.G., Landen, M., 2015. Subcortical morphometry and psychomotor function in euthymic bipolar disorder with a history of psychosis. *Brain Imaging Behav.* 9 (2), 333–341 Jun.
- Mahon, P.B., Lee, D.S., Trinh, H., et al., 2015. Morphometry of the amygdala in schizophrenia and psychotic bipolar disorder. *Schizophr. Res.* 164 (1–3), 199–202 May.
- Mamah, D., Barch, D.M., 2011. Diagnosis and classification of the schizophrenia spectrum disorders. In: Ritsner, M.S. (Ed.), *Handbook of Schizophrenia Spectrum Disorders*. Springer, New York.
- Mamah, D., Wang, L., Barch, D., de Erausquin, G.A., Gado, M., Csernansky, J.G., 2007. Structural analysis of the basal ganglia in schizophrenia. *Schizophr. Res.* 89 (1–3), 59–71 Jan.
- Mamah, D., Harms, M.P., Wang, L., et al., 2008. Basal ganglia shape abnormalities in the unaffected siblings of schizophrenia patients. *Biol. Psychiatry* 64 (2), 111–120 Jul 15.
- Mamah, D., Barch, D.M., Csernansky, J.G., 2009. Neuromorphometric measures as endophenotypes of schizophrenia spectrum disorders. In: Ritsner, M.S. (Ed.), *Neuropsychiatric Biomarkers, Endophenotypes, and Genes: Promises, Advances and Challenges*. Springer, Netherlands, pp. 87–122.
- Mamah, D., Harms, M.P., Barch, D., Styner, M., Lieberman, J.A., Wang, L., 2012. Hippocampal shape and volume changes with antipsychotics in early stage psychotic illness. *Front Psychiatry* 3, 96.
- McCarley, R.W., Wible, C.G., Frumin, M., et al., 1999. MRI anatomy of schizophrenia. *Biol. Psychiatry* 45 (9), 1099–1119 May 1.
- Meshul, C.K., Casey, D.E., 1989. Regional, reversible ultrastructural changes in rat brain with chronic neuroleptic treatment. *Brain Research* 489 (2), 338–346 Jun 12.
- Meshul, C.K., Stallbaumer, R.K., Taylor, B., Janowsky, A., 1994. Haloperidol-induced morphological changes in striatum are associated with glutamate synapses. *Brain Research* 648 (2), 181–195 Jun 20.
- Mohanakrishnan Menon, P., Nasrallah, H.A., Lyons, J.A., Scott, M.F., Liberto, V., 2003. Single-voxel proton MR spectroscopy of right versus left hippocampi in PTSD. *Psychiatry Res.* 123 (2), 101–108 Jun 30.
- Nguyen, M.N., Hori, E., Matsumoto, J., Tran, A.H., Ono, T., Nishijo, H., 2013. Neuronal responses to face-like stimuli in the monkey pulvinar. *Eur. J. Neurosci.* 37 (1), 35–51 Jan.
- Oertel-Knochel, V., Knochel, C., Matura, S., et al., 2012. Cortical-basal ganglia imbalance in schizophrenia patients and unaffected first-degree relatives. *Schizophr. Res.* 138 (2–3), 120–127 Jul.
- O'Mara, S., 2005. The subiculum: what it does, what it might do, and what neuroanatomy has yet to tell us. *J. Anat.* 207 (3), 271–282 Sep.
- Ong, D., Walterfang, M., Malhi, G.S., Styner, M., Velakoulis, D., Pantelis, C., 2012. Size and shape of the caudate nucleus in individuals with bipolar affective disorder. *Aust. N. Z. J. Psychiatry* 46 (4), 340–351 Apr.
- Ottens, M., Meeter, M., 2015. Hippocampal structure and function in individuals with bipolar disorder: a systematic review. *J. Affect. Disord.* 174, 113–125 Mar 15.
- Perneger, T.V., 1998. What's wrong with Bonferroni adjustments. *BMJ* 316 (7139), 1236–1238 Apr 18.
- Qiu, A., Wang, L., Younes, L., et al., 2009. Neuroanatomical asymmetry patterns in individuals with schizophrenia and their non-psychotic siblings. *Neuroimage* 47 (4), 1221–1229 Oct 1.
- Qiu, A., Tuan, T.A., Woon, P.S., Abdul-Rahman, M.F., Graham, S., Sim, K., 2010. Hippocampal-cortical structural connectivity disruptions in schizophrenia: an integrated perspective from hippocampal shape, cortical thickness, and integrity of white matter bundles. *Neuroimage* 52 (4), 1181–1189 Oct 1.
- Qiu, A., Gan, S.C., Wang, Y., Sim, K., 2013. Amygdala-hippocampal shape and cortical thickness abnormalities in first-episode schizophrenia and mania. *Psychol. Med.* 43 (7), 1353–1363 Jul.
- Quigley, S.J., Scanlon, C., Kilmartin, L., et al., 2015. Volume and shape analysis of subcortical brain structures and ventricles in euthymic bipolar I disorder. *Psychiatry Res.* 233 (3), 324–330 Sept.
- Rosa-Neto, P., Doudet, D.J., Cumming, P., 2004. Gradients of dopamine D1- and D2/3-binding sites in the basal ganglia of pig and monkey measured by PET. *NeuroImage* 22 (3), 1076–1083 Jul.
- Saalman, Y.B., Kastner, S., 2013. A role for the pulvinar in social cognition (commentary on Nui et al.). *Eur. J. Neurosci.* 37 (1), 33–34 Jan.
- See, R.E., Chapman, M.A., Meshul, C.K., 1992. Comparison of chronic intermittent haloperidol and raclopride effects on striatal dopamine release and synaptic ultrastructure in rats. *Synapse* 12 (2), 147–154 Oct.
- Seidman, L.J., Faraone, S.V., Goldstein, J.M., et al., 2002. Left hippocampal volume as a vulnerability indicator for schizophrenia: a magnetic resonance imaging morphometric

- study of nonpsychotic first-degree relatives. *Arch. Gen. Psychiatry* 59 (9), 839–849 Sep.
- Shenton, M.E., Gerig, G., McCarley, R.W., Szekely, G., Kikinis, R., 2002. Amygdala-hippocampal shape differences in schizophrenia: the application of 3D shape models to volumetric MR data. *Psychiatry Res.* 115 (1–2), 15–35 Aug 20.
- Shepherd, A.M., Laurens, K.R., Matheson, S.L., Carr, V.J., Green, M.J., 2012. Systematic meta-review and quality assessment of the structural brain alterations in schizophrenia. *Neurosci. Biobehav. Rev.* 36 (4), 1342–1356 Apr.
- Sherman, S.M., Guillery, R.W., 2013. *Functional Connections of Cortical Areas: New View from the Thalamus*. MIT Press, Cambridge, Massachusetts.
- Shihabuddin, L., Buchsbaum, M.S., Hazlett, E.A., et al., 1998. Dorsal striatal size, shape, and metabolic rate in never-medicated and previously medicated schizophrenics performing a verbal learning task. *Arch. Gen. Psychiatry* 55 (3), 235–243 Mar.
- Shu, X.J., Xue, L., Liu, W., et al., 2013. More vulnerability of left than right hippocampal damage in right-handed patients with post-traumatic stress disorder. *Psychiatry Res.* 212 (3), 237–244 Jun 30.
- Small, S.A., Schobel, S.A., Buxton, R.B., Witter, M.P., Barnes, C.A., 2011. A pathophysiological framework of hippocampal dysfunction in ageing and disease. *Nat. Rev. Neurosci.* 12 (10), 585–601 Oct.
- Smith, M.J., Wang, L., Cronenwett, W., Mamah, D., Barch, D.M., Csernansky, J.G., 2011. Thalamic morphology in schizophrenia and schizoaffective disorder. *J. Psychiatr. Res.* 45 (3), 378–385 Mar.
- Staal, W.G., Hulshoff Pol, H.E., Schnack, H.G., Hoogendoorn, M.L., Jellema, K., Kahn, R.S., 2000. Structural brain abnormalities in patients with schizophrenia and their healthy siblings. *Am. J. Psychiatry* 157 (3), 416–421 Mar.
- Stefanis, N., Frangou, S., Yakeley, J., et al., 1999. Hippocampal volume reduction in schizophrenia: effects of genetic risk and pregnancy and birth complications. *Biol. Psychiatry* 46 (5), 697–702 Sep 1.
- Styner, M., Lieberman, J.A., Pantazis, D., Gerig, G., 2004. Boundary and medial shape analysis of the hippocampus in schizophrenia. *Med. Image Anal.* 8 (3), 197–203 Sep.
- Swayze 2nd, V.W., Andreasen, N.C., Alliger, R.J., Yuh, W.T., Ehrhardt, J.C., 1992. Subcortical and temporal structures in affective disorder and schizophrenia: a magnetic resonance imaging study. *Biol. Psychiatry* 31 (3), 221–240 Feb 1.
- Taylor, J.E., Worsley, K.J., 2007. Detecting sparse signals in random fields, with an application to brain mapping. *J. Am. Stat. Assoc.* 102 (479), 913–928 Sep.
- Tepes, R., Wang, L., Miller, M.I., Falkai, P., Csernansky, J.G., 2003. Hippocampal deformities in the unaffected siblings of schizophrenia subjects. *Biol. Psychiatry* 54 (11), 1234–1240 Dec 1.
- Uranova, N.A., Orlovskaya, D.D., Apel, K., Klitsova, A.J., Haselhorst, U., Schenk, H., 1991. Morphometric study of synaptic patterns in the rat caudate nucleus and hippocampus under haloperidol treatment. *Synapse* 7 (4), 253–259 Apr.
- van Erp, T.G., Thompson, P.M., Kieseppa, T., et al., 2012. Hippocampal morphology in lithium and non-lithium-treated bipolar I disorder patients, non-bipolar co-twins, and control twins. *Hum. Brain Mapp.* 33 (3), 501–510 Mar.
- van Erp, T.G., Hibar, D.P., Rasmussen, J.M., et al., 2016. Subcortical brain volume abnormalities in 2028 individuals with schizophrenia and 2540 healthy controls via the ENIGMA consortium. *Mol. Psychiatry* (in press).
- van Groen, T., Kadish, I., Wyss, J.M., 2002. The role of the laterodorsal nucleus of the thalamus in spatial learning and memory in the rat. *Behav. Brain Res.* 136 (2), 329–337 Nov 15.
- Vernon, A.C., Natesan, S., Crum, W.R., et al., 2012. Contrasting effects of haloperidol and lithium on rodent brain structure: a magnetic resonance imaging study with post-mortem confirmation. *Biol. Psychiatry* 71 (10), 855–863 May 15.
- Verstynen, T.D., Badre, D., Jarbo, K., Schneider, W., 2012. Microstructural organizational patterns in the human corticostriatal system. *J. Neurophysiol.* 107 (11), 2984–2995 Jun.
- Wang, L., Mamah, D., Harms, M.P., et al., 2008. Progressive deformation of deep brain nuclei and hippocampal-amygdala formation in schizophrenia. *Biol. Psychiatry* 64 (12), 1060–1068 Dec 15.
- Womer, F.Y., Wang, L., Alpert, K.I., et al., 2014. Basal ganglia and thalamic morphology in schizophrenia and bipolar disorder. *Psychiatry Res.* 223 (2), 75–83 Aug 30.
- Worsley, K.J., 2005. An improved theoretical P value for SPMs based on discrete local maxima. *NeuroImage* 28 (4), 1056–1062 Dec.
- Worsley, K.J., Andermann, M., Koulis, T., MacDonald, D., Evans, A.C., 1999. Detecting changes in nonisotropic images. *Hum. Brain Mapp.* 8 (2–3), 98–101.
- Worsley, K., Taylor, J., Carbonell, F., et al. *SurfStat: a Matlab toolbox for the statistical analysis of univariate and multivariate surface and volumetric data using linear mixed effects models and random field theory*. Paper presented at: Organization for Human Brain Mapping; San Francisco, CA, 2009.
- Zierhut, K.C., Grassmann, R., Kaufmann, J., Steiner, J., Bogerts, B., Schiltz, K., 2013. Hippocampal CA1 deformity is related to symptom severity and antipsychotic dosage in schizophrenia. *Brain* 136 (Pt 3), 804–814 Mar.